Electronic Supplementary Material (ESI) for Journal of Materials Chemistry A.
This journal is © The Royal Society of Chemistry 2022

Supplementary Information

CO oxidation on $MgAl_2O_4$ supported Ir_n: Activation of lattice oxygen in the subnanometer regime and emergence of nuclearity-activity volcano

Yubing Lu,‡[a] Coogan Thompson,‡[a] Chun-Te Kuo,[a] Xiwen Zhang,[a] Adam S. Hoffman,[b] Alexey Boubnov, [b] Simon R. Bare,[b] Libor Kovarik,[c] Hongliang Xin,[a] Ayman M. Karim*[a]

a. Department of Chemical Engineering, Virginia Polytechnic Institute and State University, Blacksburg, Virginia 24060, USA

b. Stanford Synchrotron Radiation Light Source, SLAC National Accelerator Laboratory, Menlo Park, California 94025, USA

c. Institute for Integrated Catalysis, and Fundamental and Computational Science Directorate, Pacific Northwest National Laboratory, Richland, Washington 99354 USA

‡ These authors contributed equally

*E-mail: amkarim@vt.edu

Table S1. Atomic percentage size distribution of two catalysts containing Ir subnanometer clusters, $Ir_{Subnano}/MgAl_2O_4$ and $Ir_{Subnano\_Ir4}/MgAl_2O_4$.

Sample	0.1-0.3 nm	0.3-0.5 nm	0.5-0.7 nm	0.7-0.9 nm	0.9-1 nm
$Ir_{Subnano}/MgAl_2O_4$ before reaction	28%	6%	30%	29%	7%
$Ir_{Subnano}/MgAl_2O_4$ after reaction	25%	2%	31%	32%	10%
$Ir_{Subnano\_Ir4}/MgAl_2O_4$ before reaction	13%	24%	44%	21%	0%

Table S2. Size distribution of $MgAl_2O_4$ supported Ir samples measured from STEM.

Sample	Ir weight Loading	Percentage of single atoms (SA)	0.3-0.7 nm	0.7-1 nm	> 1nm	Major species
$Ir_{Subnano}/MgAl_2O_4$	0.05%	28%	36%	36%	0%	Subnano
$Ir_{Subnano\_Ir4}/MgAl_2O_4$	0.1%	13%	68%	21%	0%	Subnano
Ir_{NP} $/MgAl_2O_4$	0.2%	2%	0%	22%	76%	NP
$Ir_{SA}/MgAl_2O_4$	0.0025%	~100%	0%	0%	0%	SA
$Ir_{SA+NP}/MgAl_2O_4$	1%	35%	1%	18%	46%	SA+NP
$Ir_{NP}/MgAl_2O_4$ (1wt.%)	1%	16%	0%	7%	77%	Mostly NP

Table S3. Summary of EXAFS modeling of $Ir_{Subnano}/MgAl_2O_4$ catalysts under different conditions.

Sample	Ir subnano H_2 30 °C	Ir subnano CO 30 °C	Ir subnano CO 160 °C	Ir subnano O_2 30 °C	Ir NP He 30 °C[1]
$N_{Ir\text{-}Ir}$	3.5±1.3	3.3±1.8	3.3±1.8	2.7±1.9	6.6±0.4
$N_{Ir\text{-}C}$		0.6±0.5	0.6±0.5	– [a]	
$N_{Ir\text{-}O}$	3.2±0.5	3.3±0.6	3.3±0.6	4.1±0.6	0.2±0.1
$N_{Ir\text{-}Al/Mg}$	3.9±0.9	3.8±0.8	3.8±0.8	3.4±1.0	0.2±0.1
$R_{Ir\text{-}Ir}$ (Å)	2.65±0.01	2.66±0.05	2.64±0.06	2.62±0.03	2.689±0.002
$R_{Ir\text{-}C}$ (Å)		1.88±0.1	1.95±0.1		
$R_{Ir\text{-}O(CO)}$ (Å)		3.04±0.1	3.08±0.1		
$R_{Ir\text{-}O}$ (Å)	2.04±0.01	2.06±0.02	2.07±0.02	2.02±0.01	2.06±0.04
$R_{Ir\text{-}Al/Mg}$ (Å)	2.95±0.01	2.95±0.04	2.94±0.05	2.94±0.02	2.93±0.04
$\sigma^2_{Ir\text{-}Ir} \times 10^3$ (Å^2)	5±3	6±5	8±7	9±9	5.8±0.3
$\sigma^2_{Ir\text{-}C} \times 10^3$ (Å^2)		0±9	0±9		
$\sigma^2_{Ir\text{-}O(CO)} \times 10^3$ (Å^2)		2±10	3±10		
$\sigma^2_{Ir\text{-}O} \times 10^3$ (Å^2)	4±2	3±3	1±1	3±2	1±7
$\sigma^2_{Ir\text{-}Al/Mg} \times 10^3$ (Å^2)	3±6	2±4	1±4	2±4	0±5
$\Delta E_{0\ Ir\text{-}Ir}$ (eV)	1±7	1±7	1±7	1±7	7.0±0.7
$\Delta E_{0\ Ir\text{-}C}$ (eV)		8±4	8±4		
$\Delta E_{0\ Ir\text{-}O}$ (eV)	8±4	8±4	8±4	8±4	10±5
$\Delta E_{0\ Ir\text{-}Al/Mg}$ (eV)	8±4	8±4	8±4	8±4	10±5
Reduced χ^2	103	103	103	103	16
R-factor	0.0039	0.0039	0.0039	0.0039	0.0003

[a] The fit was not reliable with scattering paths for Ir-CO. However, CO was observed in DRIFTS (Figure 2 in the manuscript)

Notation: N, coordination number of absorber-backscatterer pair; R, radial absorber-backscatterer distance; σ^2, the mean square displacement of the half-path length and represents the stiffness of the bond for a single scattering path, ΔE_0, correction to the threshold energy.

Table S4. CO volumetric chemisorption on different samples.

Sample	Ir weight loading	Gas	Qty. adsorbed μmol/g	Gas:Ir
$Ir_{Subnano}/MgAl_2O_4$	0.05%	CO	2.38	CO:Ir = 0.9:1
Ir_{NP} /$MgAl_2O_4$	0.2%	CO	9.4	CO:Ir = 0.9:1
$Ir_{SA+NP}/MgAl_2O_4$	1% $Ir/MgAl_2O_4$	CO	72.3	CO:Ir =1.4:1
$Ir_{NP}/MgAl_2O_4$ (1wt.%)	1% $Ir/MgAl_2O_4$	CO	53	CO:Ir =1:1

Table S5. TOF of Ir catalysts with different ways of active site normalization.

Sample	Active site	Active Ir/surface Ir	TOF (normalized with surface Ir)[a]	TOF (normalized with the active Ir)[a]
Ir NP	Surface Ir site	1:1	1.75	1.75
Ir subnano	Interfacial site	~ 0.53:1[b]	5.74	9.33
Ir SA	Ir atom	1:1	1.26	1.26

a. measurement condition: 0.3 kPa CO, 10 kPa O_2, at 155 °C.

b. The active site is estimated based on a hemispherical Ir cluster model with a 0.77 nm radius. The cluster has 14 atoms in total, 13 surface Ir atoms, and 8 perimeter Ir atom at the Ir-$MgAl_2O_4$ interface. The ratio of active Ir (i.e. interfacial/perimeter Ir) to surface Ir sites is estimated as 0.62:1.

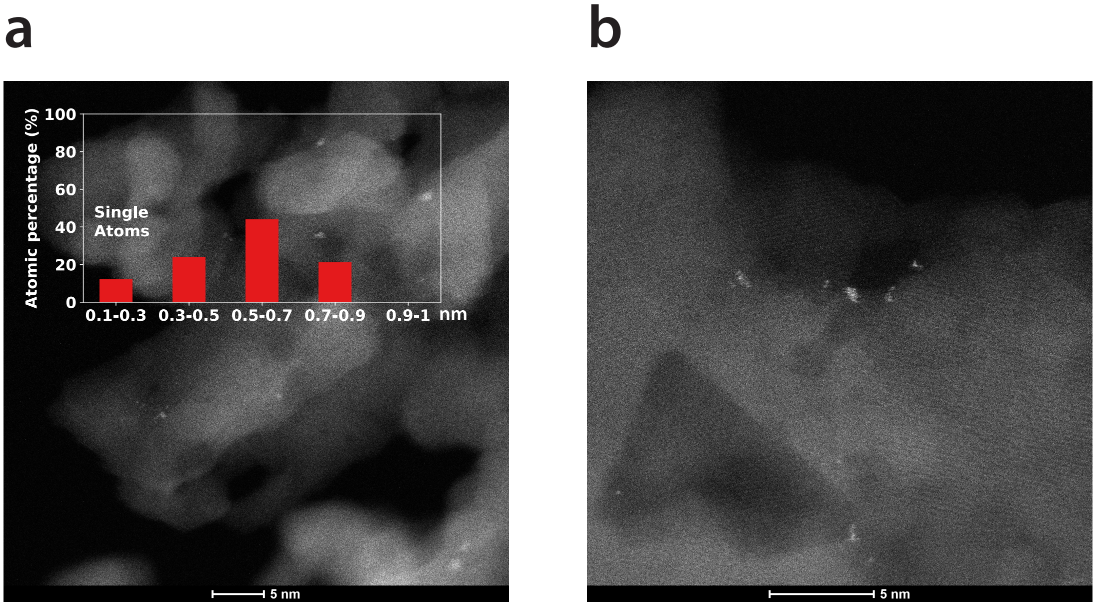

Figure S1. HAADF-STEM images of the $Ir_{Subnano\_Ir4}/MgAl_2O_4$. Histogram obtained from multiple images is shown in (a).

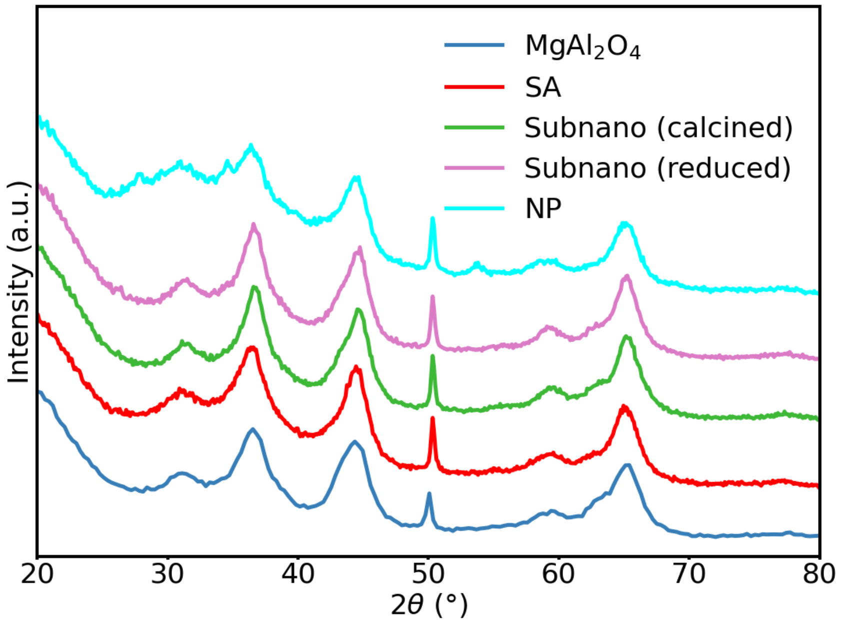

Fig. S2. XRD for the samples in this work. The support ($MgAl_2O_4$) was calcined at 500 °C as described in the synthesis section. The preparation of the $Ir_{SA}/MgAl_2O_4$ and $Ir_{NP}/MgAl_2O_4$ were reported in our previous work.[19] The preparation of the $Ir_{subnano}/MgAl_2O_4$ is described in the synthesis section. The calcined sample was taken after the ex-situ calcination while the reduced sample was taken after ex-situ reduction (700 °C in H_2 followed by exposure to air). The peak at $2\theta = 50$ ° is a background peak from the sample compartment/holder.

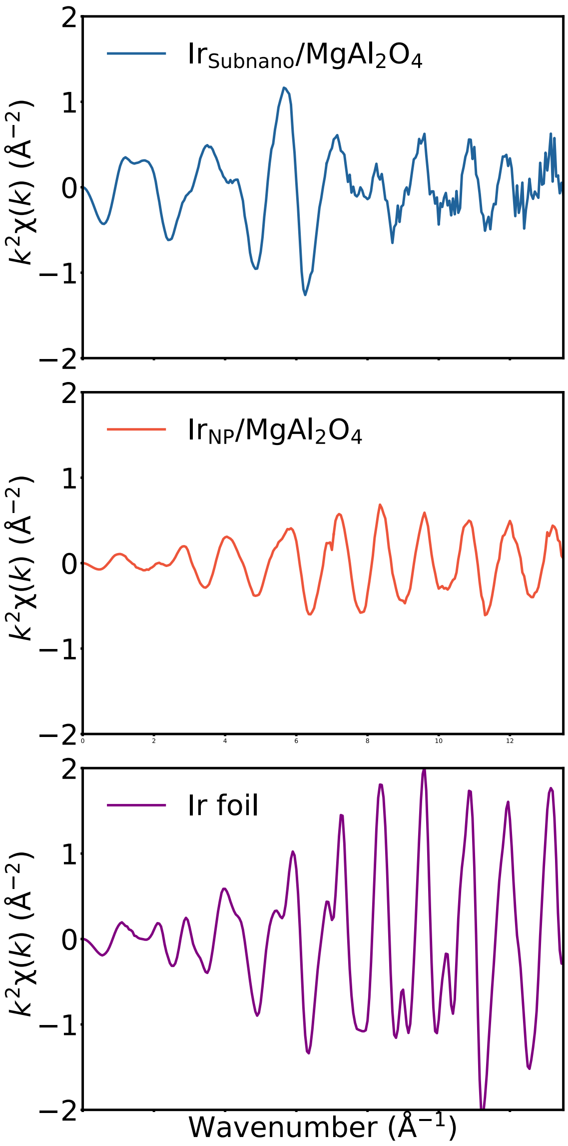

Figure S3. Ir L_3-edge X-ray absorption spectroscopy k-space data measured on $Ir_{Subnano}/MgAl_2O_4$ after H_2 pretreatment, $Ir_{NP}/MgAl_2O_4$ after H_2 pretreatment and Ir foil.

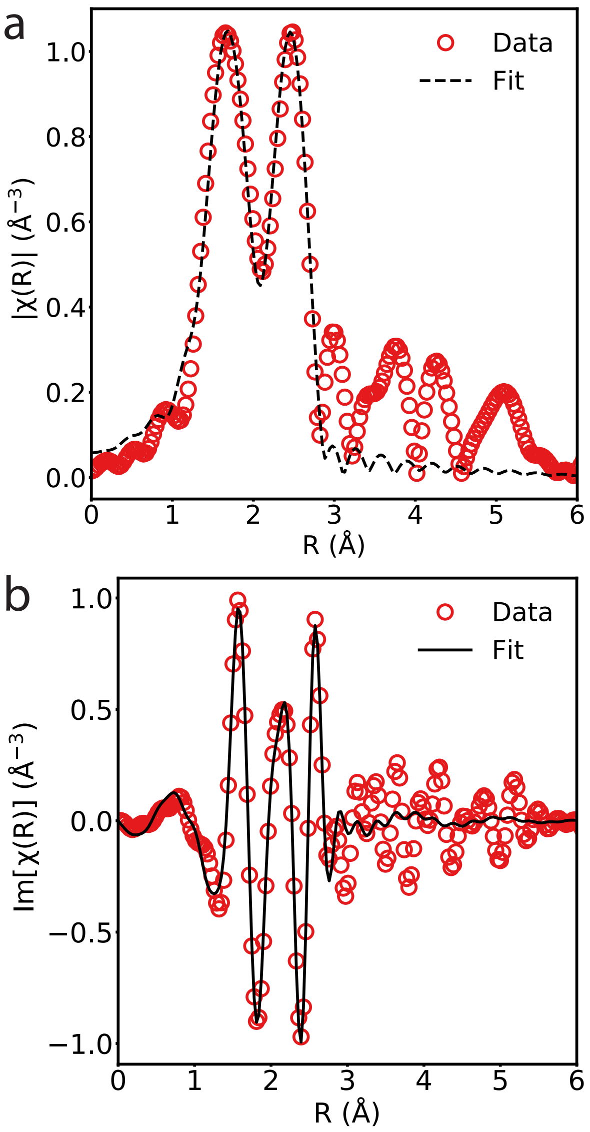

Figure S4. Ir L_3-edge Fourier transformed EXAFS spectra and fit of $Ir_{Subnano}/MgAl_2O_4$ after H_2 pretreatment. **(a)** magnitude and **(b)** imaginary part of the Fourier transformed k^2-weighted $\chi(k)$ data (Δk= 2.5-12 Å^{-1}) (Δk = 2.7-16 Å^{-1}). The r-range for the fit was 1.3-3.0 Å

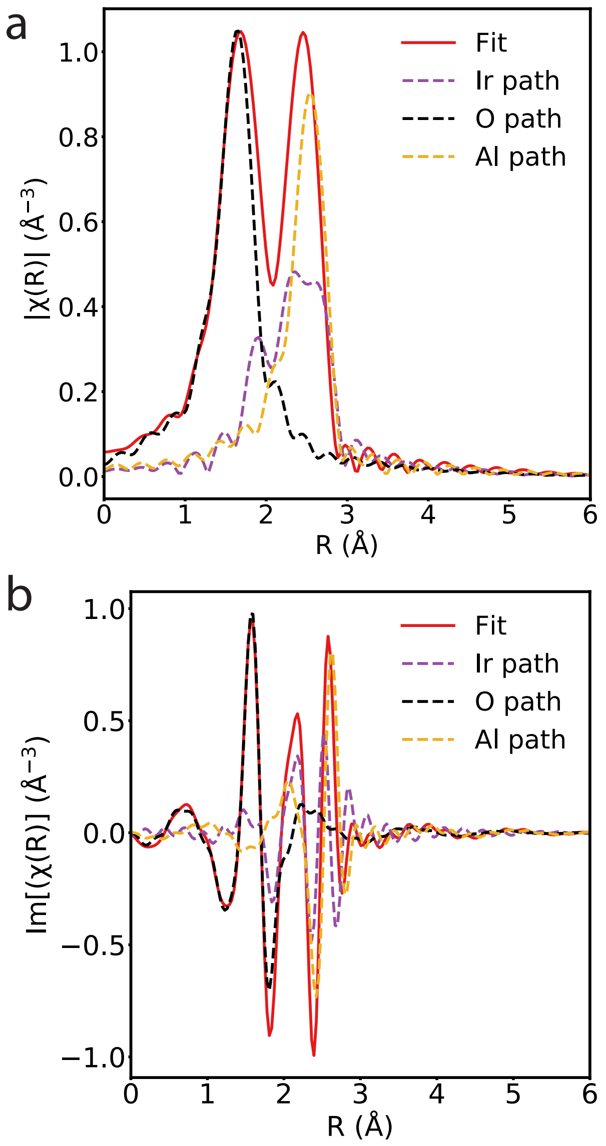

Figure S5. EXAFS fit to $Ir_{Subnano}/MgAl_2O_4$ after H_2 pretreatment. Contribution of different scattering paths. (Ir path = Ir–Ir; O path = Ir–O; Al path = Ir–Al) (a) R space magnitude and (b) R space imaginary.

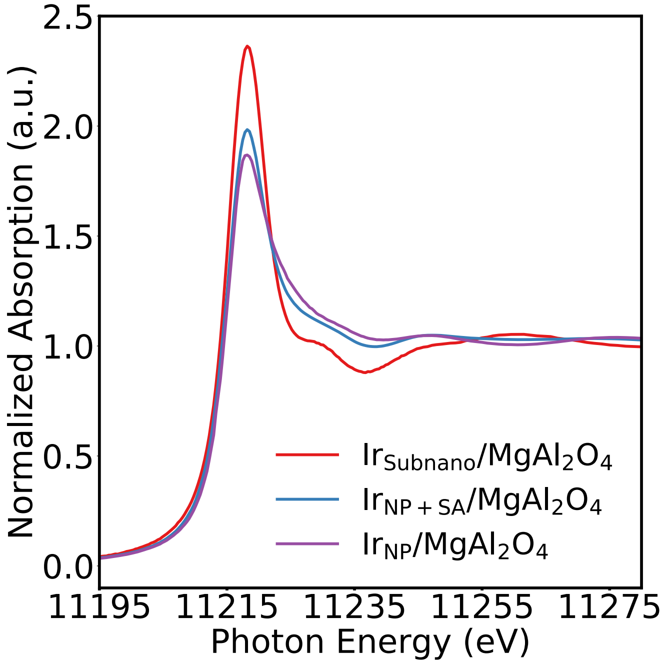

Figure S6. Ir L_3-edge X-ray absorption near edge spectroscopy characterizing $Ir_{Subnano}/MgAl_2O_4$, $Ir_{NP+SA}/MgAl_2O_4$ and $Ir_{NP}/MgAl_2O_4$ (1wt.%).

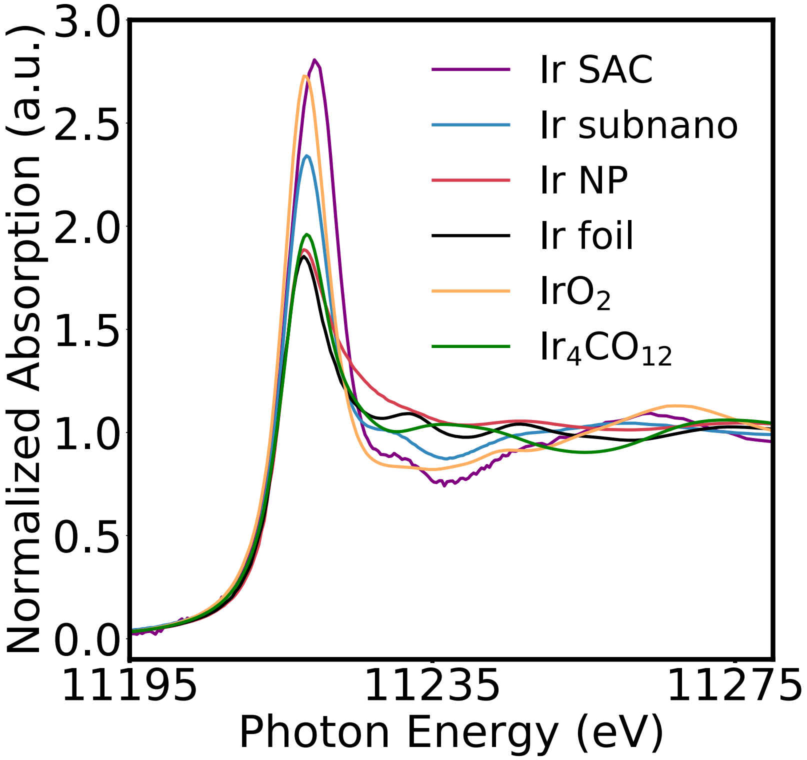

Figure S7. Ir L3-edge X-ray absorption near edge spectroscopy characterizing $Ir_{SA}/MgAl_2O_4$, $Ir_{subnano}/MgAl_2O_4$, $Ir_{NP}/MgAl_2O_4$, and Ir references include Ir foil, IrO_2 and Ir_4CO_{12}. All three $Ir/MgAl_2O_4$ catalysts were measured after H_2 pretreatment.

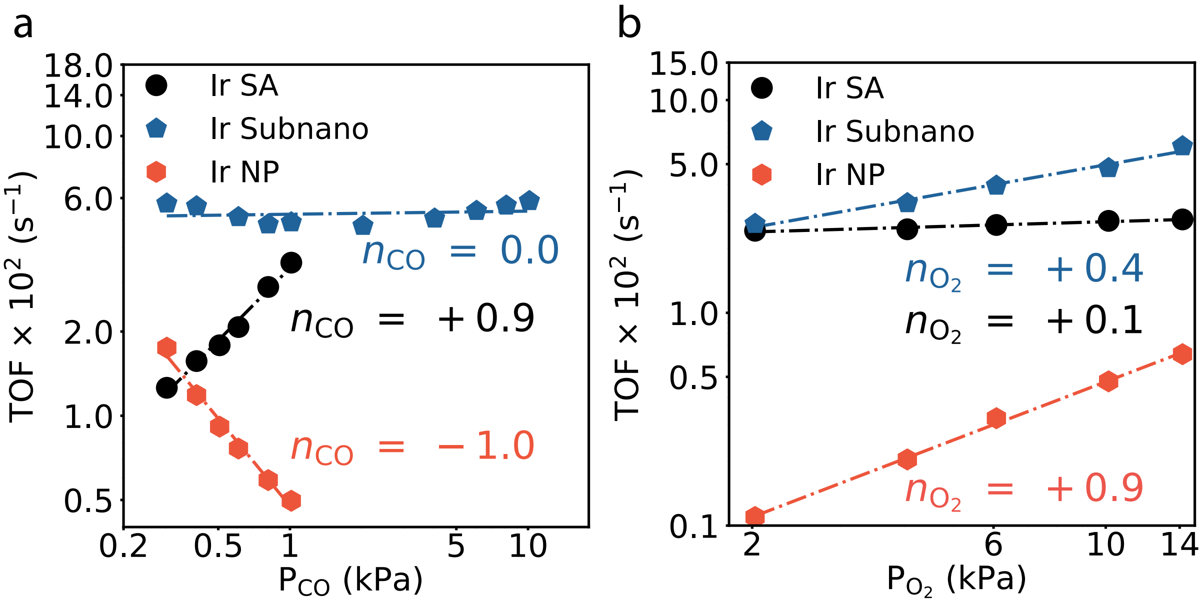

Figure S8. Effect of (a) CO partial pressure and (b) O_2 partial pressure on turnover frequency (TOF) on $Ir_{Subnano}/MgAl_2O_4$ (blue), $Ir_{SA}/MgAl_2O_4$ (black)[2] and $Ir_{NP}/MgAl_2O_4$ (red)[2] (a) O_2 partial pressure = 10 kPa, CO partial pressure = 0.3-10 kPa. Measured at 155 °C. (b) O_2 partial pressure = 2-14 kPa, CO partial pressure = 1 kPa. Measured at 155 °C.

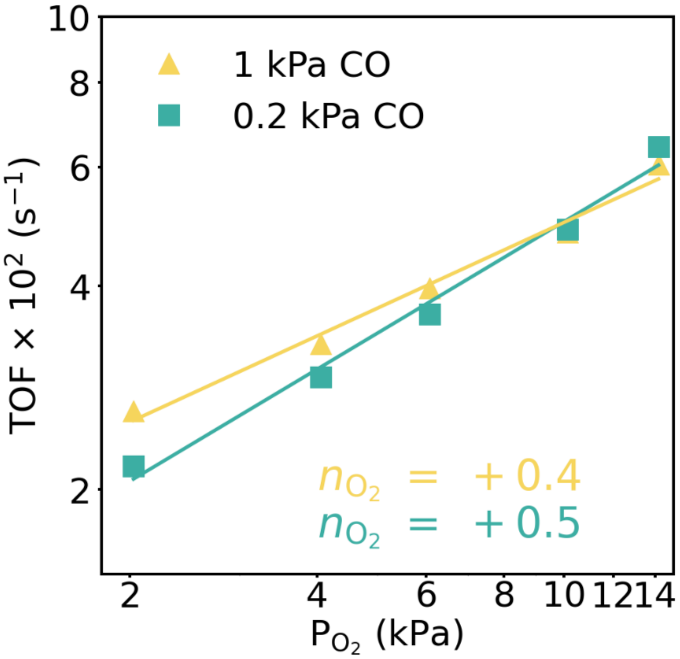

Figure S9. Effect of O_2 pressure on turnover frequency (TOF) on $Ir_{Subnano}/MgAl_2O_4$ measured at two CO partial pressures: 1 and 0.2 kPa. O_2 partial pressure was varied between 2-14 kPa. Measured at 155 °C.

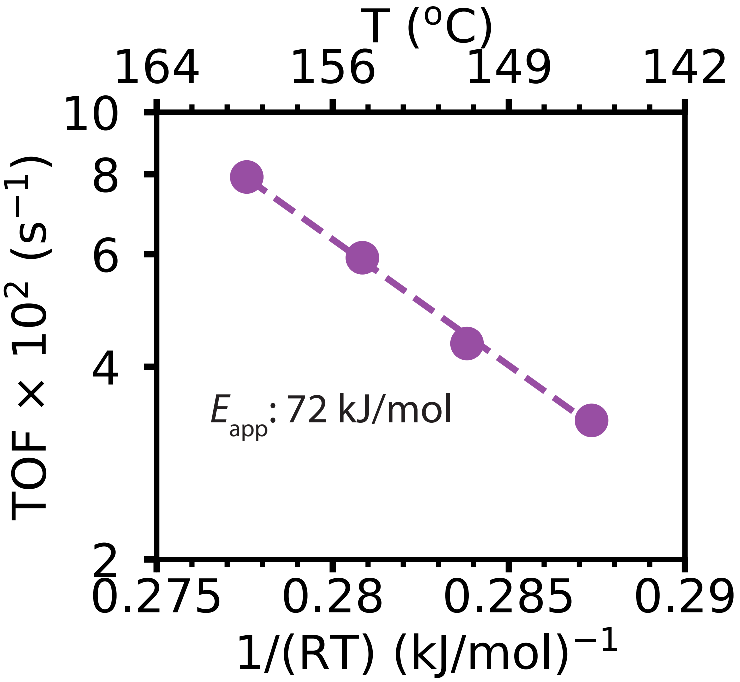

Figure S10. Effect of temperature on turnover frequency (TOF) on $Ir_{Subnano}/MgAl_2O_4$. O_2 partial pressure was kept at 10 kPa, CO partial pressure was measured at 1 kPa. Measured between 143 - 160 °C.

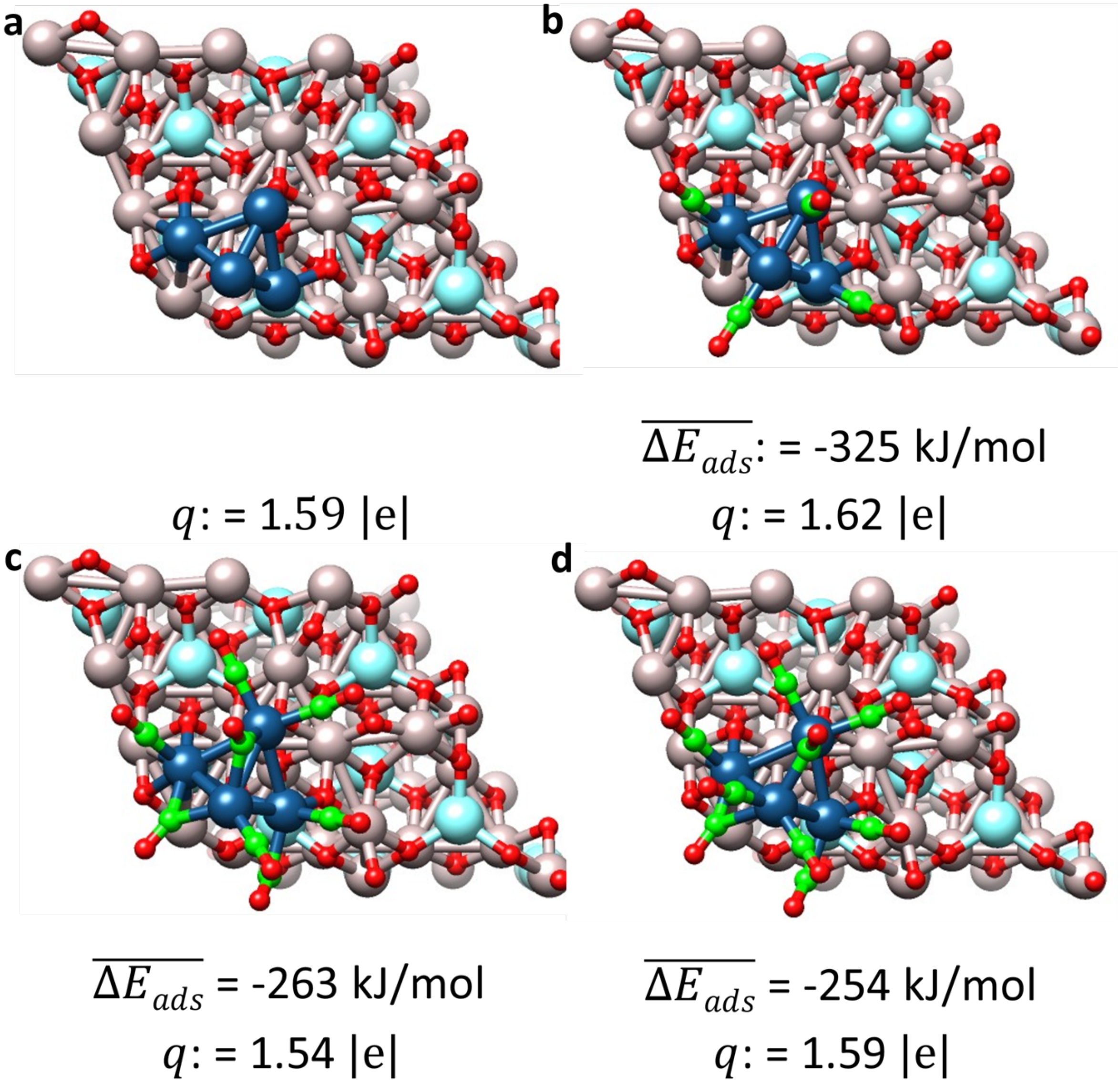

Figure S11. DFT optimized structures representing various levels of CO coverage: 0, 4, 8, and 9 COs. 9 CO is treated as full coverage. ΔE_{ads} is the average binding energy of the COs on the structure and q is the average Bader charge for the structures.

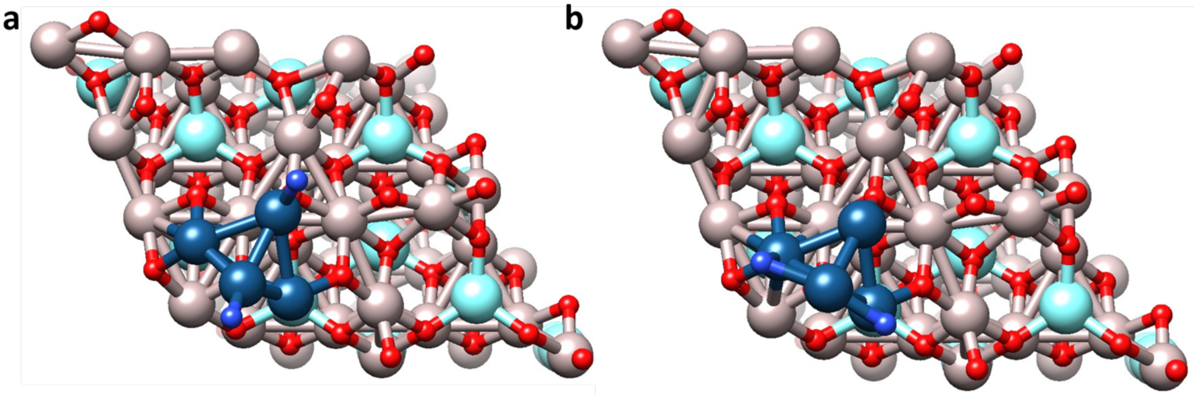

Figure S12. Examples of structures used to calculate the initial dissociative binding energy of O_2 on the Ir_4 cluster.

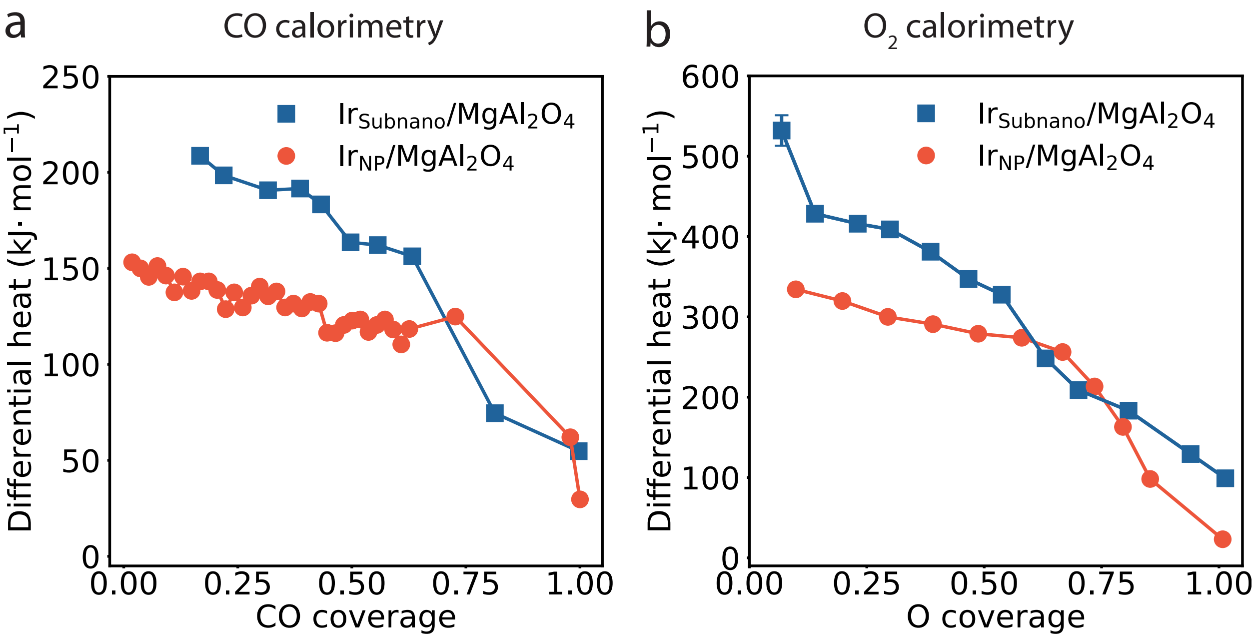

Figure S13. CO (a) and O_2 (b) calorimetry of $Ir_{Subnano}/MgAl_2O_4$ and the $Ir_{NP}/MgAl_2O_4$ (1 wt.%). Measured at 30 ºC for both CO and O_2 calorimetry. Differential heat (kJ mol^{-1}) in (a) and (b) is normalized by mol of CO and O_2 adsorbed, respectively. The coverage of 1 is defined as the point when the heat reached ~40 kJ/mol.

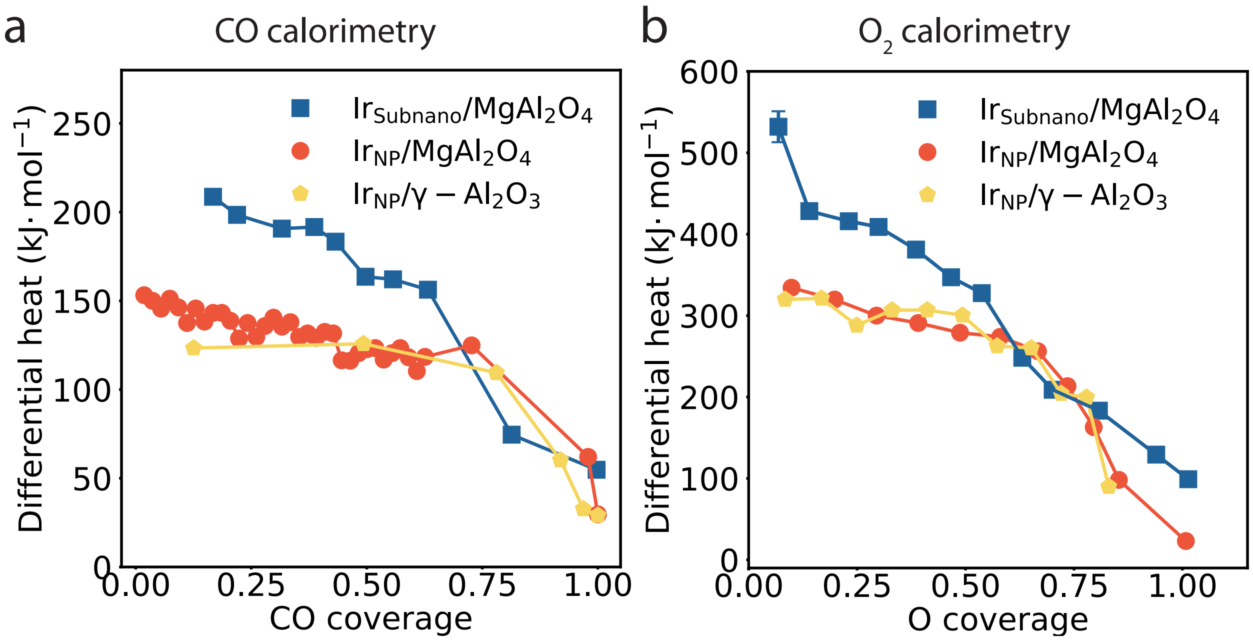

Figure S14. CO and O_2 calorimetry of three Ir catalysts with different particle sizes. Ir_{NP}/γ-Al_2O_3 serves as a Ir standard with larger particle size. Representative TEM images of Ir nanoparticle in Ir_{NP}/γ-Al_2O_3 with average size 5-12 nm is shown in Fig. S20. Differential heat (kJ mol^{-1}) is normalized with per mol of CO and O_2 adsorbed, respectively. The coverage of 1 is defined as the point when the heat reached ~40 kJ/mol.

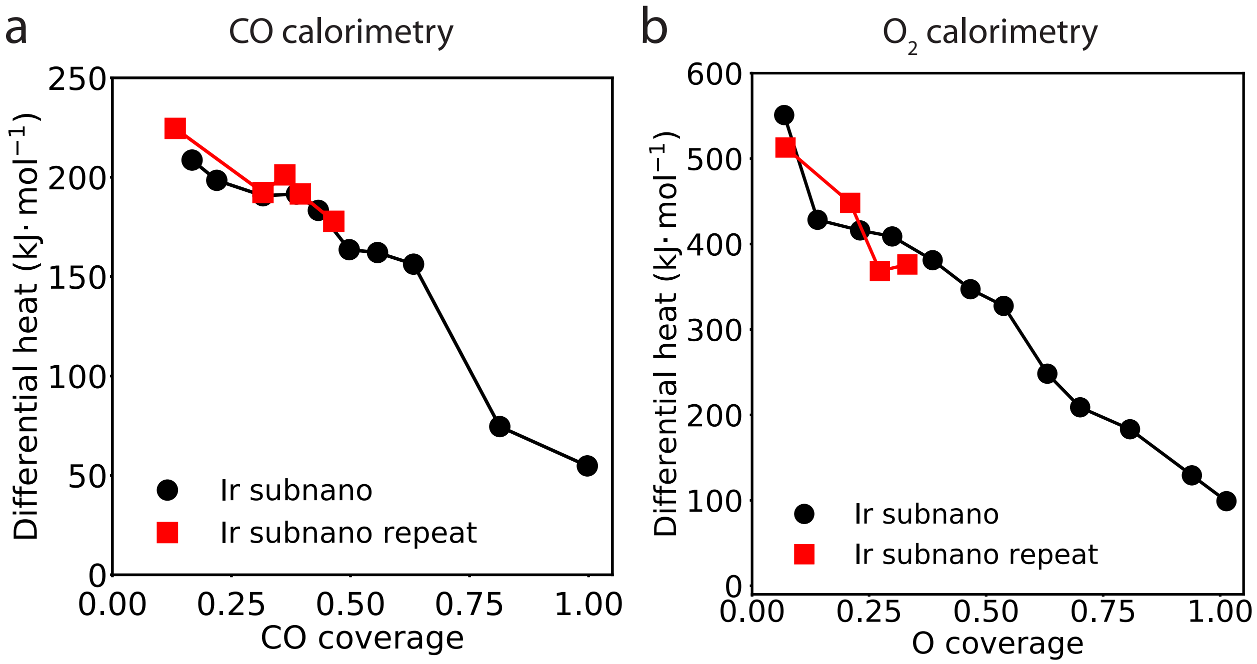

Figure S15. CO (a) and O_2 calorimetry of $Ir_{Subnano}/MgAl_2O_4$ repeated on two different batches. Measured at 30 °C for both CO and O_2 calorimetry. Mol of CO in (a) and mol of O in (b) are normalized with mol of surface Ir of the catalyst obtained with CO chemisorption. Differential heat (kJ mol^{-1}) is normalized with per mol of CO and O_2 adsorbed, respectively. The coverage of 1 is defined as the point when the heat reached ~40 kJ/mol.

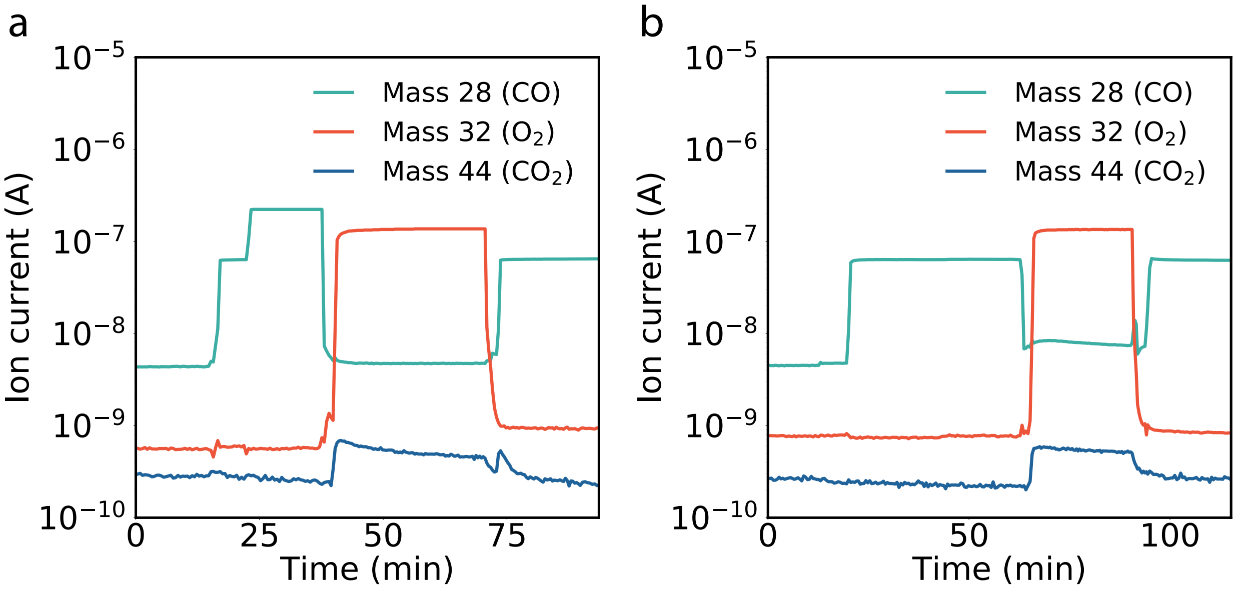

Figure S16. Mass spectrometry results of the gas concentration from the reactor effluent at 30 °C during EXAFS experiment on (a) $Ir_{Subnano}/MgAl_2O_4$ (b) $Ir_{Subnano\_Ir4}/MgAl_2O_4$. (a) Flowed 1 kPa and then 4 kPa CO, 4 kPa O_2, and 1kPa CO in sequence on $Ir_{Subnano}/MgAl_2O_4$. (b) Flowed 1 kPa CO, 4 kPa O_2, and 1 kPa CO in sequence on $Ir_{Subnano\_Ir4}/MgAl_2O_4$.

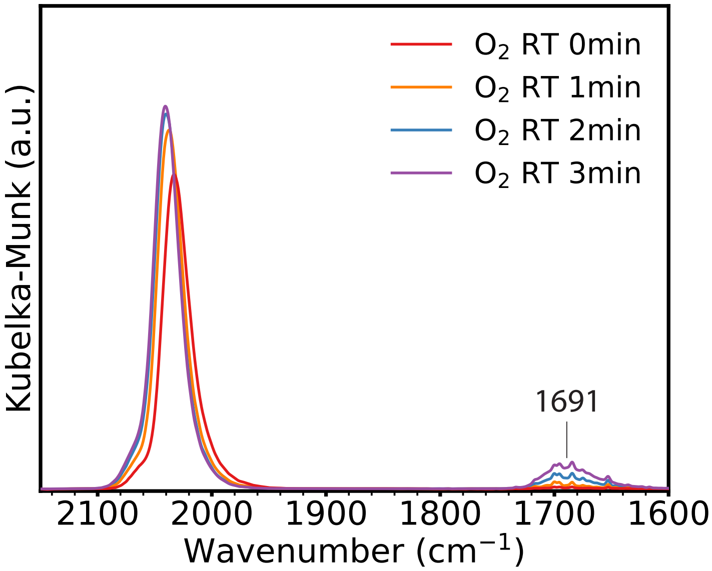

Figure S17. *In-situ* DRIFTS spectra characterizing $Ir_{Subnano}/MgAl_2O_4$ during O_2 (1 kPa) flow at room temperature after pretreatment and CO chemisorption at room temperature. Spectra was collected every 1 min.

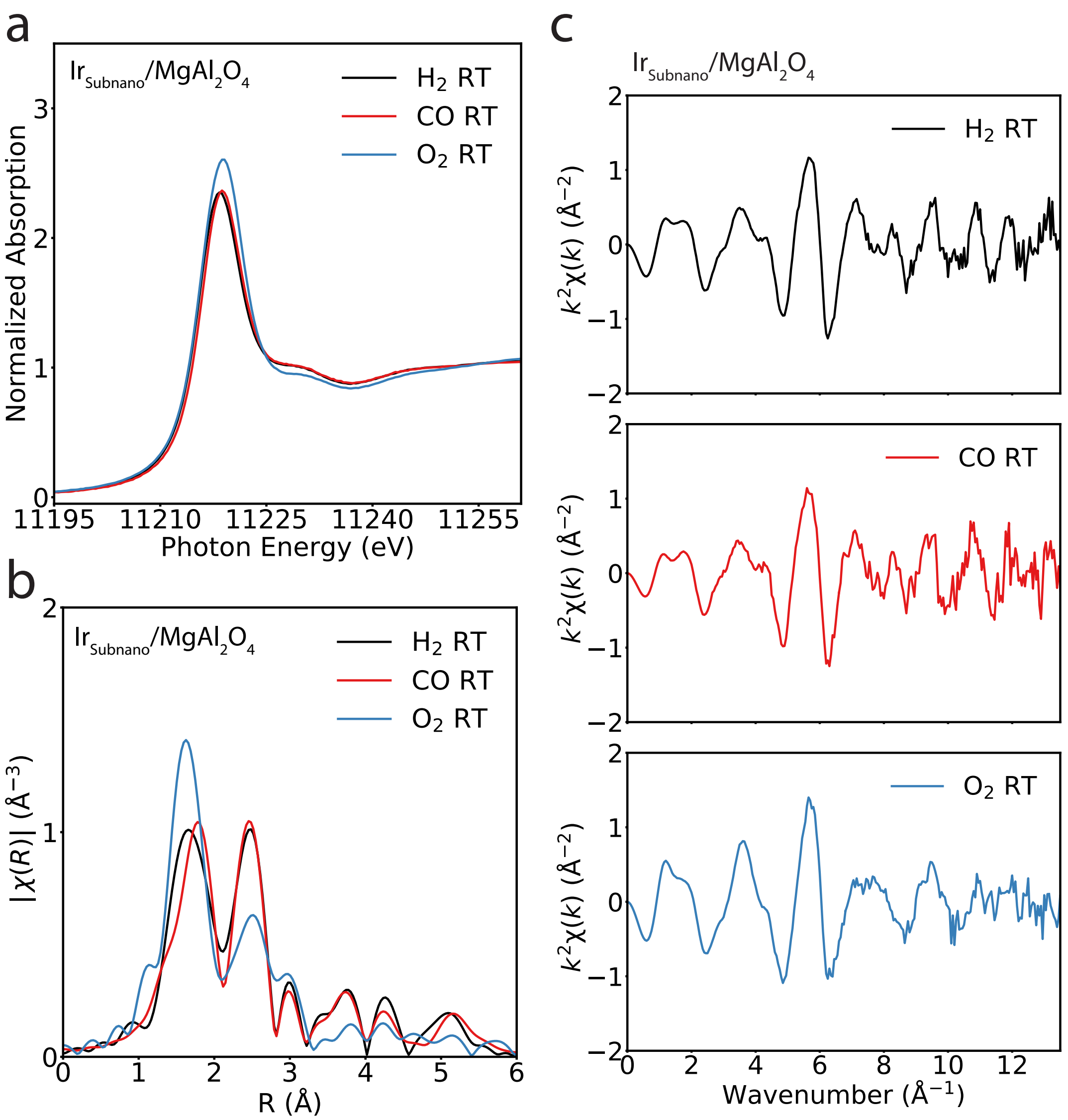

Figure S18. Ir L_3-edge X-ray absorption spectroscopy of Ir$_{Subnano}$/MgAl$_2$O$_4$ under H_2/CO/O_2 flow at room temperature. (a) XANES of Ir$_{Subnano}$/MgAl$_2$O$_4$ after H_2 pretreatment (20 kPa) and measured at room temperature, and then flow CO (1 kPa) at room temperature followed by O_2 (1kPa) at room temperature. (b) EXAFS magnitude of the Fourier transformed k^2-weighted $\chi(k)$ data measured on Ir$_{Subnano}$/MgAl$_2$O$_4$ after H_2 pretreatment (20 kPa) and measured at room temperature, and then flow CO (1 kPa) at room temperature followed by O_2 (1kPa) at room temperature. Δk = 2.6-12.5 Å^{-1}. (c) k-space data measured on Ir$_{Subnano}$/MgAl$_2$O$_4$ after H_2 pretreatment (20 kPa) and measured at room temperature, and then flow CO (1 kPa) at room temperature followed by O_2 (1kPa) at room temperature.

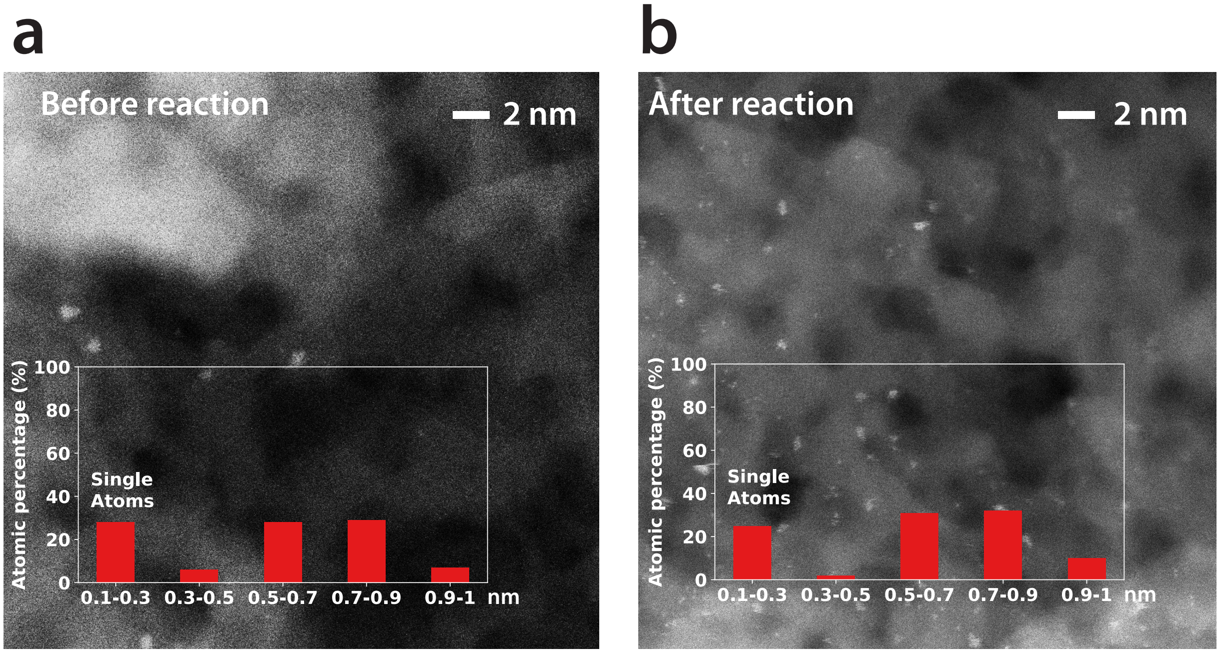

Figure S19. HAADF-STEM images of the $Ir_{Subnano\_Ir4}/MgAl_2O_4$ before and after the reaction. Histograms were obtained by measuring Ir clusters from multiple images.

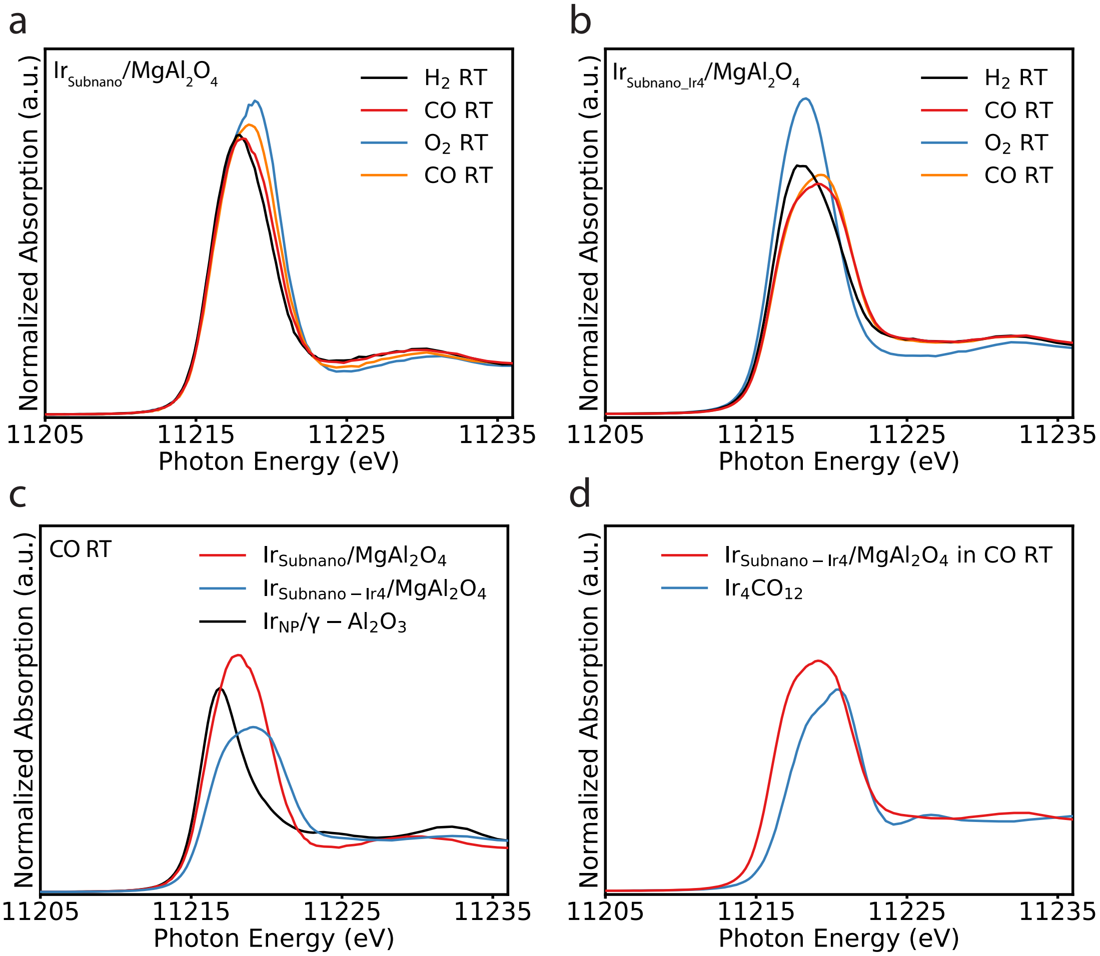

Figure S20. HERFD-XANES at Ir L_3-edge characterizing $Ir_{Subnano}/MgAl_2O_4$, $Ir_{Subnano\_Ir4}/MgAl_2O_4$ and the $Ir_4(CO)_{12}$ standard. $Ir_{Subnano}/MgAl_2O_4$ and $Ir_{Subnano\_Ir4}/MgAl_2O_4$ represent $MgAl_2O_4$ supported Ir subnanometer clusters with different size distributions. See Table S1 for size distribution. (a) HERFD-XANES spectra of $Ir_{Subnano}/MgAl_2O_4$ after H_2 pretreatment and measured at room temperature (black), flowed CO (1 kPa) at room temperature (red), flowed O_2 (1 kPa) at room temperature (blue), and then flowed CO (1 kPa) at room temperature (orange). (b) HERFD-XANES spectra of $Ir_{Subnano}/MgAl_2O_4$ after H_2 pretreatment and measured at room temperature (black), flowed CO (1 kPa) at room temperature (red), flowed O_2 (1 kPa) at room temperature (blue), and then flowed CO (1 kPa) at room temperature (orange). (c) HERFD-XANES spectra of $Ir_{Subnano}/MgAl_2O_4$ after the first CO flow at room temperature as shown in a, $Ir_{Subnano\_Ir4}/MgAl_2O_4$ after the first CO flow at room temperature as shown in b, and the Ir_{NP}/γ-Al_2O_3

sample with the average particle size between 5-8 nm. (d) HERFD-XANES spectra of $Ir_{Subnano\_Ir4}/MgAl_2O_4$ after the first CO flow at room temperature as shown in b, and $Ir_4(CO)_{12}$ standard.

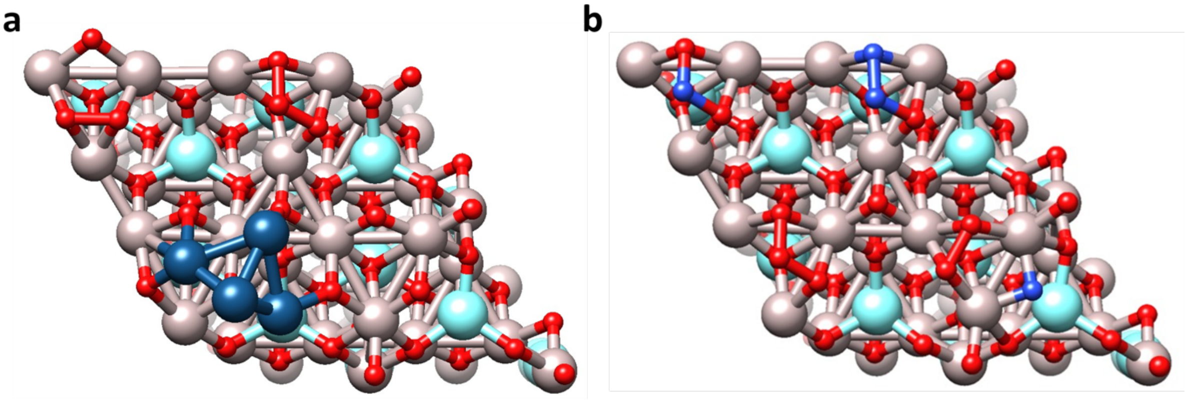

Figure S21. (a) Most stable Ir_4 surface species on $MgAl_2O_4$ (111) before changes to surface termination were considered. Dark blue represents Ir. (b) Optimized surface structure for $MgAl_2O_4$ (111)[2, 3] before the addition of Ir_4. The light blue Os in (b) were removed after the addition of the Ir_4 cluster (cluster not shown in (b) for clarity) as the Ir_4 cluster decreased the oxygen vacancy formation energy considerably (220 to 174 kJ/mol). The Os were chosen as their oxygen vacancy formation energy was below 1 eV. The surface energy was recalculated to arrive at the state used for the CO addition (Figure S9a).

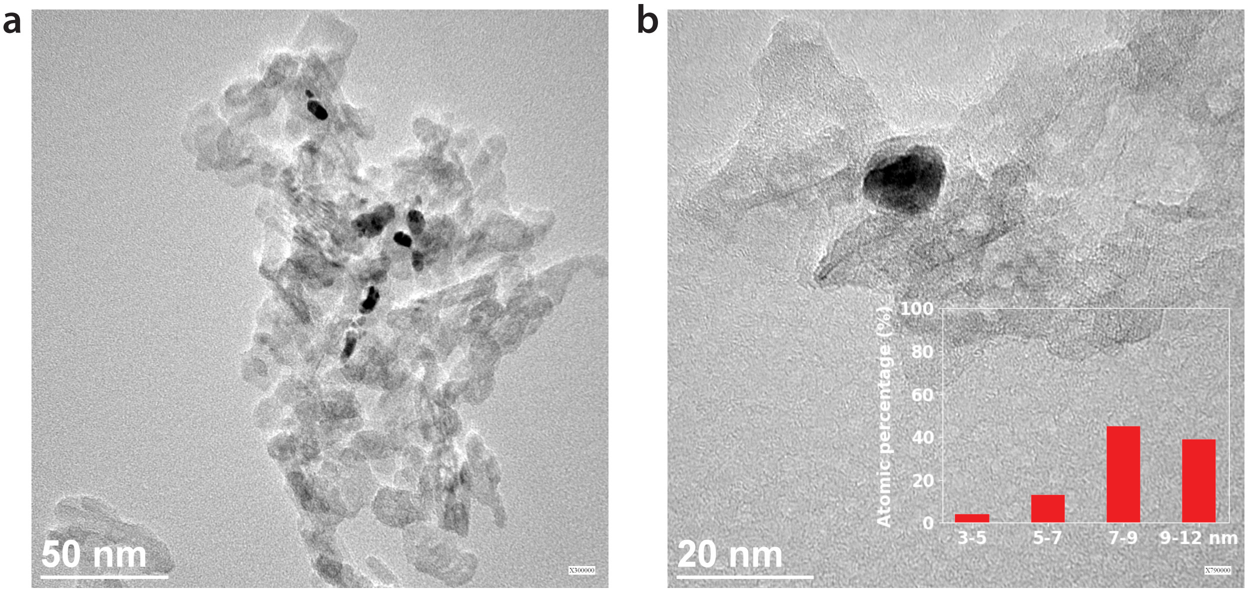

Figure S22. Representative TEM images of the Ir_{NP}/γ-Al_2O_3 sample before and after the reaction. Histogram was obtained by measuring nanoparticles from multiple images.

Derivation of the rate equation

Here we assume that the Ir(CO)* dominates the Ir clusters and O* dominates the interfacial support sites

Steps:

$$CO_{(g)} + Ir^* \underset{k_{-1}}{\overset{k_1}{\leftrightarrow}} Ir(CO)^*$$

$$O_{2(g)} + \# \underset{k_{-2}}{\overset{k_2}{\leftrightarrow}} O_2^{\#}$$

$$Ir(CO)^* + O_2^{\#} \overset{k_3}{\rightarrow} CO_{2(g)} + Ir^* + O^{\#}$$

$$Ir(CO)^* + O^{\#} \overset{k_4}{\rightarrow} CO_{2(g)} + Ir^* + \#$$

The equations:

$$[Ir(CO)^*] + [Ir^*] = 1$$

$$[O_2^{\#}] + [O^{\#}] + [\#] = 1$$

$$\frac{\partial[Ir(CO)^*]}{\partial t} = k_1 P_{CO}[Ir^*] - k_{-1}[Ir(CO)^*] - k_3[Ir(CO)^*][O_2^{\#}] - k_4[Ir(CO)^*][O^{\#}] = 0$$

$$\frac{\partial[O_2^{\#}]}{\partial t} = k_2 P_{O_2}[\#] - k_{-2}[O_2^{\#}] - k_3[Ir(CO)^*][O_2^{\#}] = 0$$

$$\frac{\partial[O^{\#}]}{\partial t} = k_3[Ir(CO)^*][O_2^{\#}] - k_4[Ir(CO)^*][O^{\#}] = 0$$

$$rate = k_4[Ir(CO)^*][O^{\#}]$$

We assume that the surface is fully covered by CO thus $[Ir(CO)^*] = 1$. Note that this assumption means we have no need for the $\frac{\partial[Ir(CO)^*]}{\partial t}$ term. Plugging in the Ir site balance:

$$[Ir(CO)^*] + [Ir^*] = 1$$

$$[Ir(CO)^*] = 1$$

$$[O_2^{\#}] + [O^{\#}] + [\#] = 1$$

$$k_2 P_{O_2}[\#] - k_{-2}[O_2^\#] - k_3[O_2^\#] = 0$$

$$k_3[O_2^\#] - k_4[O^\#] = 0$$

$$rate = k_4[O^\#]$$

We also assume that the surface vacancy site is dominated by O^*.

$$[O_2^\#] + [O^\#] + [\#] = 1$$

$$[O^\#] + [\#] = 1$$

Solving for $[O_2^\#]$ and plugging it in:

$$k_3[O_2^\#] - k_4[O^\#] = 0$$

$$[O_2^\#] = \frac{k_4}{k_3}[O^\#]$$

$$[O^\#] + [\#] = 1$$

$$k_2 P_{O_2}[\#] - \frac{k_{-2}k_4}{k_3}[O^\#] - k_4[O^\#] = 0$$

$$rate = k_4[O^\#]$$

Solving for $[O^\#]$ and plugging it in:

$$k_2 P_{O_2}[\#] - \frac{k_{-2}k_4}{k_3}[O^\#] - k_4[O^\#] = 0$$

$$[O^\#] = \frac{k_2 P_{O_2}}{\frac{k_{-2}k_4}{k_3} + k_4}[\#]$$

$$\frac{k_2 P_{O_2}}{\frac{k_{-2}k_4}{k_3} + k_4}[\#] + [\#] = 1$$

$$rate = \frac{k_2 P_{O_2}}{\frac{k_{-2}}{k_3} + 1}[\#]$$

Solving the surface site balance and plugging in:

$$\frac{k_2 P_{O_2}}{\frac{k_{-2}k_4}{k_3} + k_4}[\#] + [\#] = 1$$

$$[\#] = \frac{1}{1 + \frac{k_2 P_{O_2}}{\frac{k_{-2}k_4}{k_3} + k_4}}$$

$$rate = \frac{k_2 P_{O_2}}{\frac{k_{-2}}{k_3} + 1}\left(\frac{1}{1 + \frac{k_2 P_{O_2}}{\frac{k_{-2}k_4}{k_3} + k_4}}\right)$$

$$rate = \frac{\frac{k_2 P_{O_2}}{\frac{k_{-2}}{k_3} + 1}}{1 + \frac{k_2 P_{O_2}}{\frac{k_{-2}k_4}{k_3} + k_4}}$$

Simplifying the fractions:

$$rate = \frac{k_2 k_3 k_4 P_{O_2}}{k_4(k_{-2} + k_3) + k_2 k_3 P_{O_2}}$$

This gives two regimes a positive order one ($[*]$ dominant) and zero order ($[O^*]$ dominant).

zero order ($[O^*]$ dominant, $\frac{k_2 P_{O_2}}{\frac{k_{-2}k_4}{k_3}+k_4} \gg 1$)

$$rate = \frac{\frac{k_2 P_{O_2}}{\frac{k_{-2}}{k_3}+1}}{1+\frac{k_2 P_{O_2}}{\frac{k_{-2}k_4}{k_3}+k_4}}$$

$$rate = \frac{\frac{k_2 P_{O_2}}{\frac{k_{-2}}{k_3}+1}}{\frac{k_2 P_{O_2}}{\frac{k_{-2}k_4}{k_3}+k_4}}$$

$$rate = k_4$$

positive order ($[*]$ dominant, $\frac{k_2 P_{O_2}}{\frac{k_{-2}k_4}{k_3}+k_4} \ll 1$)

$$rate = \frac{\frac{k_2 P_{O_2}}{\frac{k_{-2}}{k_3}+1}}{1+\frac{k_2 P_{O_2}}{\frac{k_{-2}k_4}{k_3}+k_4}}$$

$$rate = \frac{\frac{k_2 P_{O_2}}{\frac{k_{-2}}{k_3}+1}}{1}$$

$$rate = \frac{k_2 k_3}{k_{-2}+k_3} P_{O_2}$$

If the system is half covered:

$$[O^*] = [*]$$

$$\frac{k_2 P_{O_2}}{\frac{k_{-2}k_4}{k_3}+k_4} = 1$$

$$O_2\ order = \frac{\partial \ln(rate)}{\partial \ln P_{O_2}} = \frac{P_{O_2}}{rate}\frac{\partial(rate)}{\partial P_{O_2}}$$

$$= \frac{P_{O_2}}{\frac{k_2 k_3 k_4 P_{O_2}}{k_4(k_{-2}+k_3)+k_2 k_3 P_{O_2}}}\frac{\partial}{\partial P_{O_2}}\left(\frac{k_2 k_3 k_4 P_{O_2}}{k_4(k_{-2}+k_3)+k_2 k_3 P_{O_2}}\right)$$

$$= \frac{\left(k_4(k_{-2}+k_3)+k_2 k_3 P_{O_2}\right)}{\left(k_4(k_{-2}+k_3)+k_2 k_3 P_{O_2}\right)^2}\left(k_4(k_{-2}+k_3)+k_2 k_3 P_{O_2} - k_2 k_3 P_{O_2}\right)$$

$$= \frac{k_4(k_{-2}+k_3)}{k_4(k_{-2}+k_3)+k_2 k_3 P_{O_2}}$$

Applying the half-covered condition:

$$\frac{k_2 P_{O_2}}{\frac{k_{-2}k_4}{k_3} + k_4} = 1$$

$$k_2 k_3 P_{O_2} = k_4(k_{-2} + k_3)$$

$$O_2\ order = \frac{k_4(k_{-2} + k_3)}{k_4(k_{-2} + k_3) + k_4(k_{-2} + k_3)} = \frac{1}{2}$$

References

1. Y. Lu, C. Kuo, L. Kovarik, A. S. Hoffman, A. Boubnov, D. M. Driscoll, J. R. Morris, S. R. Bare and A. M. Karim, *J. Catal.*, 2019, **378**, 121-130.
2. Y. Lu, J. Wang, L. Yu, L. Kovarik, X. Zhang, A. S. Hoffman, A. Gallo, S. R. Bare, D. Sokaras, T. Kroll, V. Dagle, H. Xin and A. M. Karim, *Nat. Catal.*, 2019, **2**, 149-156.
3. Q. X. Cai, J. G. Wang, Y. Wang and D. H. Mei, *J. Phys. Chem. C*, 2016, **120**, 19087-19096.